Am J Transl Res 2019;11(1):87-105
www.ajtr.org /ISSN:1943-8141/AJTR0075486

Original Article

NVP-BEZ235-induced autophagy as a potential therapeutic approach for multiple myeloma

Yongyong Ma[1,2*], Zhouxiang Jin[3*], Kang Yu[1], Qifa Liu[2]

[1]Department of Hematology, The First Affiliated Hospital of Wenzhou Medical University, 2 Nanbai Xiang, Wenzhou 325000, China; [2]Department of Hematology, Nanfang Hospital, Southern Medical University, Guangzhou 510010, China; [3]Department of Hepatobiliary Surgery, The Second Affiliated Hospital and Yuying Children's Hospital of Wenzhou Medical University, 109#, Xueyuan Western Road, Wenzhou 325027, China. [*]Equal contributors.

Received March 5, 2018; Accepted June 8, 2018; Epub January 15, 2019; Published January 30, 2019

Abstract: Background: The PI3K/Akt/mTOR pathway is constitutively activated in human multiple myeloma (MM) cell lines and in freshly isolated plasmocytes from patients with MM. The mTOR signaling pathway has been designated an attractive anti-tumor target in multiple myeloma. NVP-BEZ235, a novel, dual class I PI3K/mTOR inhibitor, is an imidazoquinoline derivative. NVP-BEZ235 binds to the ATP-binding clefts of PI3K and mTOR kinase, thereby inhibiting their activities. Increasing evidence shows that NVP-BEZ235 is able to effectively and specifically reverse the hyperactivation of the PI3K/mTOR pathway, resulting not only in potent antiproliferative and antitumor activities in a broad range of cancer cell lines and experimental tumors but also in autophagy. Method: The antitumor, apoptosis, and autophagy effects of NVP-BEZ235 were measured in three MM cell lines, two leukemia cell lines, and primary CD138+ myeloma cells from MM patients and nude mouse MM models. In addition, the relationships between autophagy, cell death and apoptosis induced by NVP-BEZ235 were analyzed in MM cells. Furthermore, we explored the mechanism of autophagy induced by NVP-BEZ235 in MM cells. Results: NVP-BEZ235 inhibited proliferation and induced apoptosis and autophagy in MM cells and in primary MM cells from patients and nude mouse MM models. Autophagy played an important role in the cell death and apoptosis of MM cell lines induced by NVP-BEZ235, and the mechanism involved the mTOR2-Akt-FOXO3a-BNIP3 pathway. Conclusions: In this study, NVP-BEZ235 showed the strongest antitumor and autophagy induction activity. Moreover, the mechanism involved the mTOR2-Akt-FOXO3a-BNIP3 pathway. Our study lays a theoretical foundation for NVP-BEZ235 clinical application.

Keywords: NVP-BEZ235, multiple myeloma, autophagy, mechanism, mTOR, apoptosis, pathway

Introduction

Multiple myeloma (MM) is a malignancy of terminal B cells and represents nearly 2% of all cancers [1, 2]. The PI3K/Akt/mTOR pathway is constitutively activated in human myeloma cell lines and in freshly isolated plasmocytes from patients with MM. Mammalian target of rapamycin (mTOR) is a downstream serine/threonine kinase of the PI3K/AKT pathway that integrates signals from the microenvironment such as cytokines, growth factors, and nutrients to regulate multiple cellular processes, including mRNA translation, autophagy, metabolism, growth and survival [3-5]. mTOR operates in two distinct multiprotein complexes, mTORC1 and mTORC2. Sharing mTOR kinase as a common catalytic subunit, mTORC1 controls cell growth and mTORC2 modulates cell survival and drug resistance. The mTOR signaling pathway has been found to be deregulated in multiple myeloma and has been designated an attractive anti-tumor target [6-9]. Rapamycin has demonstrated in vitro activity against MM cell lines as a single agent and in combination with the immunomodulatory drug CC-5013. Exposure to rapamycin or temsirolimus prevents the proliferation of PTEN- and RAS-mutated myeloma cell lines [10, 11]. Temsirolimus was shown to inhibit the growth of human myeloma cell lines by inducing G1 cell cycle arrest, apoptosis, and tumor angiogenesis. In a murine xenograft model of MM, temsirolimus demonstrated a dose-dependent inhibition of proliferation and angiogenesis and induced tumor cell apoptosis [12, 13]. In a NOD-SCID mouse model of diffuse MM, everolimus suppressed MM tumor burden and led to a

longer survival time. Several clinical studies of mTOR inhibitors are ongoing in MM patients. In a phase I/II open-label trial of everolimus, 17 patients with relapsed or refractory MM were enrolled after at least two lines of previous treatment [14-16].

NVP-BEZ235, a novel, dual class I PI3K/mTOR inhibitor, is an imidazoquinoline derivative [17]. NVP-BEZ235 binds to the ATP-binding clefts of PI3K and mTOR kinase, thereby inhibiting their activities. Increasing evidence shows that NVP-BEZ235 is able to effectively and specifically reverse the hyperactivation of the PI3K/mTOR pathway, resulting in potent antiproliferative and antitumor activities in a broad range of cancer cell lines and experimental tumors [18-21]. In breast cancer cells, NVP-BEZ235 blocks the activation of the downstream effectors of mTORC1/2, including Akt, S6 and 4E-BP1. Additionally, NVP-BEZ235 shows greater antiproliferative activity than the allosteric selective mTOR inhibitor everolimus in all cancer cell lines tested. In a xenograft model of BT474-derived breast cancer cells overexpressing either the p110α H1047R oncogenic mutation or empty vector, NVP-BEZ235 significantly inhibits the tumor growth of both xenografts. Consistently, NVP-BEZ235 at nanomolar concentrations suppresses phosphorylation of Akt, S6K and 4E-BP1 and inhibits cell growth in a panel of cancer cells, including human glioma, osteosarcoma, Ewing's sarcoma, and rhabdomyosarcoma. Inhibition of PI3K/AKT/mTOR signaling can not only inhibit the proliferation of tumor cells but also induce autophagy [22, 23]. Autophagy is a catabolic process that maintains cellular homeostasis and reduces diverse stressors through lysosomal recycling of unnecessary and damaged cell components [4]. This process is also observed to antagonize antitumor efficacy in colon cancer sw480 cells, via apoptotic inhibition [24, 25]. We aimed to investigate the inhibitory effects and autophagy of NVP-BEZ235 in multiple myeloma and its relationships with cell death and apoptosis and study the role of autophagy in the NVP-BEZ235 treatment of multiple myeloma.

Materials and methods

Reagents

NVP-BEZ235 and chloroquine were obtained from Selleck Chemicals (TX, USA). 3MA and Acridine orange (AO), trypan blue, dimethylsulfoxide (DMSO), 3-(4,5-dimethyl-2-thiazolyl)-2, and 5-diphenyl-2H-tetrazolium bromide (MTT) were obtained from Sigma Chemical Co. (St. Louis, MO, USA). Anti-LC3B, anti-p62, anti-ATG5, anti-mTOR, anti-p-mTOR, anti-AKT, anti-p-AKT, anti-p70S6K, anti-p-p70S6K, anti-beclin1, anti-LC3-II/I, anti-Caspase-3 and anti-Caspase-9 were purchased from Cell Signaling Technology (Beverly, MA, USA).

Cell lines and primary MM cells

Human MM U266, RPMI8226, KM3 cell lines, acute monocytic leukemia THP-1 cells and acute promyelocytic leukemia HL60 cells were obtained from the American Type Culture Collection, and cells were cultured in RPMI-1640 supplemented with 10% fetal bovine serum (FBS). Cells were cultured at 37°C in a humidified atmosphere with 5% CO_2. Those cells under logarithmical growth phase were used for further experiments. Bone marrow samples were acquired from 3 patients with MM who gave informed consent in accordance with the Declaration of Helsinki. The protocols were approved by the Ethics Committee of Wenzhou Medical University. CD138+ cells were separated with an LS+ column and a magnetic separator according to the manufacturer's instructions (Miltenyi Biotech). The purity of CD138+ cells (> 90%) was confirmed by flow cytometry and CD138-phycoerythrin staining. The viability of the cells was regularly greater than 95% by trypan blue exclusion. CD138+ cells were cultured in RPMI-1640 supplemented with 10% FBS. NVP-BEZ235 was dissolved as a stock solution at 0.03 M in dimethyl sulfoxide and then further diluted in serum-free medium of RPMI-1640 just before use. Cell viability was determined by the trypan-blue exclusion assay, and the growth inhibition rate was calculated according to the percentage of viable cell number of treated cells against untreated cells.

MTT assay

MM cells were plated in 96-well plates at a density of 1×10^4 cells/well, cultured, and then treated with NVP-BEZ235 at different concentrations (0, 100 nM, 200 nM, 300 nM, 400 nM) for 0, 12, 24, 48 and 72 h dissolved by DMSO for 24, 48 and 72 h, respectively. Cells treated with DMSO as the solvent were used as the control. After treatment, 10 μL MTT of 5 mg/mL

was then added into each well, and all plates were further incubated for 4 h. Next, 100 μL of DMSO was used to dissolve the dark blue crystals. Finally, the plates were read on a Spectra Max MS (MDC, Sunnyvale, CA), at the wavelength of 570 nm. The original survival ratio of the vehicle control group was set as 100%, and the relative survival ratio of NVP-BEZ235-treated cells was defined as a percentage of the absorbance value of NVP-BEZ235 treated cells against that of vehicle control cells. The assay was performed in triplicate wells, and each experiment was repeated three times.

Transmission electron microscopy

Cells were fixed overnight in 2.5% glutaraldehyde. Next, they were washed with PBS three times and put in 1% osmium tetroxide at 4°C for 1 hour. Ethanol series and 100% acetone were used to dehydrate the cells. Then, the cells were embedded in epoxy resins. The ultrathin sections were stained with lead citrate solution and uranyl acetate and then observed under a transmission electron microscope (JEOL Ltd. Tokyo, Japan).

Acridine orange staining

During autophagy, autophagosomes fuse with lysosomes to form autophagolysosomes which can be stained with AO. MM cells seeded at 5 × 10^4 cells per well in 24-well culture plates were collected, exposed to NVP-BEZ235 (50 and 100 nM) for 12 h, and stained with 3 μl (1 μM) AO for 15 min. The cells were then washed three times with PBS, adding 30 μl anti-quencher per well; immediately observed under an inverted fluorescence microscope (Nikon Corporation, Japan); and examined with the FACSCalibur Flow Cytometry System.

Colonies formation assays

MM cells were seeded in 24-well plates; 24 h later, cells were cultured in 10% FBS for 14 days (with medium replenished after 7 days). Cells were stained with Giemsa (Sigma, St. Louis, USA) to visualize colonies.

Hoechst 33258 staining

Hoechst 33258 staining was used to investigate the changes in nuclear morphology of apoptosis, observed by fluorescence microscopy. The cells were fixed with 4% paraformaldehyde at 37°C for 10 minutes, washed with PBS and stained with 0.5 ml Hoechst 33258 in the dark for 5 min. The apoptotic cells with condensed and fragmented nuclei were counted by fluorescence microscopy.

Flow cytometric analysis

After annexin V and propidium iodide (PI) staining, cell apoptosis was detected by flow cytometry. One hundred and five cells in 500 μL of binding buffer were mixed with 5 μL of annexin V-FITC following incubation for the indicated duration, and then 5 μL of PI was added to the MM cells, which were incubated at room temperature in the dark for 1 hour. The stained cells were detected by the FACSCalibur Flow Cytometry System and data were analyzed by CellQuest software.

Quantitative real-time PCR

Total RNA was isolated using an RNA isolation kit following the manufacturer's instructions (Qiagen, Germantown, MD, USA). RNA was reverse transcribed using the SuperScript II reverse transcriptase assay (Invitrogen, Carlsbad, CA, USA). cDNA was analyzed using quantitative PCR (qPCR) with a CFX Real-Time PCR Detection System (Bio-Rad, Hercules, CA, USA). The expression of associated genes was determined by RT-PCR using the following primers: Atg5, 5'-GACAAAGATGTGCTTCGAGATGTG-3' and 5'-GTAGCTCAGATGCTCGCTCAG-3'; FOXO3a, 5'-GCGTGCCCTACTTCAAGGATAAG-3', 5'-GACCCGCATGAATCGACTATG-3'; BNIP3, 5'-GCCCACCTCGCTCGCAGACAC-3' and 5'-CAATCCGATGGCCAGCAAATGAGA-3'; β-actin, 5'-CAAGATCATTGCTCCTCCTG-3' and 5'-TCATCGTACTCCTGCTTGCT-3'. PCR reactions were carried out for 40 cycles that comprised a denaturation step at 95°C for 15 s and an annealing step at 60°C for 1 min. The amplified segments were analyzed using gel electrophoresis.

Western blotting

MM cells were washed three times in serum-free medium and then lysed with RIPA buffer (50 Mm Tris-HCl pH 7.4, 1% (v/v) Triton X-100, 1 mM EDTA, 1 mM leupeptin, 1 mM phenylmethylsulfonyl fluoride, 10 mM NaF, 1 mM Na_3VO_4). The lysates were isolated by 12% SDS-PAGE and then transferred to PVDF membranes. The membranes were probed with primary antibodies against LC3B, p62, ATG5, mTOR, p-mTOR,

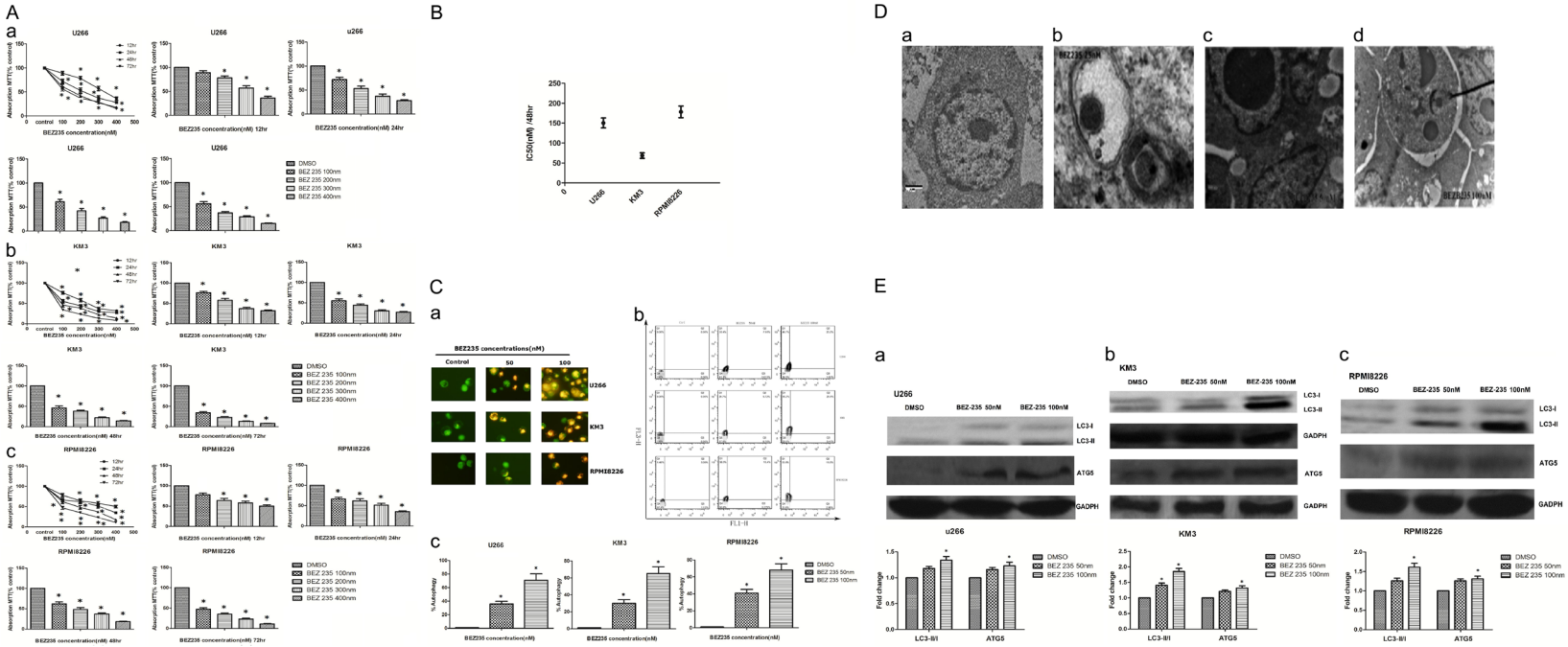

Figure 1. Autophagy, cell viability inhibition induced by NVP-BEZ235 on MM cell lines. (A) Effects of NVP-BEZ235 on viability of U266, KM3 and RPMI8226 MM cells. Human myeloma cell lines U266, KM3 and RPMI8226 were treated with NVP-BEZ235 at different concentrations (0, 100 nM, 200 nM, 300 nM and 400 nM) for 0, 12, 24, 48 and 72 h. Cell viability was detected by MTT assay. (B) IC50 of NVP-BEZ235 in U266, KM3 and RPMI8226 cell lines at 48 hours. (C) Acridine orange was used to stain AVOs in untreated or BEZ235 (50, 100 nM)-treated U266, KM3 and RPMI8226 cells for 12 hours. (a) The cells were visualized under a red filter fluorescence microscope. (b) The cells were detected by flow cytometry. (c) Autophagic ratio was calculated by measuring red/green fluorescence ratio. (D) NPV-BEZ235 induces ultrastructural features of autophagy. KM3 cells were treated with NVP-BEZ235 (0, 25, 50, 100 nM) for 12 h and processed for electron microscopy. Note the double membrane structure of the autophagic vacuoles. We indicate the presence of degrading autophagic vacuoles (AVds). N: Nucleus. (E) Effects of NVP-BEZ235 on the expression of LC3II and Atg5 in MM cells. Cells were treated with 50 nM and 100 nM NVP-BEZ235 for 12 h and (a) LC3II and Atg5 expression and the fold change in U266 cells was tested using Western blot analysis. (b) LC3II and Atg5 expression and the fold change in U266 cells was tested using Western blot analysis. (c) LC3II and Atg5 expressions and the fold change in RPMI8226 cells was tested using Western blot analysis. *Means significant difference was observed between the treated group and control ($P < 0.05$).

AKT, p-AKT, p70S6K, p-p70S6K, Caspase-3, Caspase-9 and β-actin and then incubated with secondary antibodies. Finally, the membranes were harvested with an enhanced chemiluminescence plus Western Blotting Detection System (Pierce, USA).

Small interfering RNA oligos

The 21-bp small interfering RNAs (siRNAs) were synthesized by Invitrogen and were specific against siFOXO3a, 5'-GGGCGACAGCAACAGCTCT-3' and siBNIP3, 5'-GCUACUCUCAGCAUGAGAATT-3'; scrambled control siRNA was obtained from Sangon Biotech Co., Ltd. (Shanghai, China). SiFOXO3a, siBNIP3 and scrambled siRNA were transfected into three MM cells with the aid of Hiperfect transfection reagent (Qiagen, Valencia, CA, USA).

Xenograft MM cells implantation

Male BALB/c nude mice (3-4 weeks old) were obtained from the Laboratory Animal Center of Wenzhou Medical University (Wenzhou, Zhejiang) and housed in a rodent facility under a 12-hour light-dark cycle. Two groups (DMSO, BEZ235 (30 mg/kg/d, p.o.)), each containing seven mice, were implanted with U266 cells (2×10^7 cells) via subcutaneous injection into the right forelimb region. Treatment was started after 14 days, when the tumors were approximately 5 mm in diameter. All experiments were performed in accordance with the regulations of the WMU Guide for the Care and Use of Laboratory Animals.

Evaluation of tumor volume, body weight, general situation and transmission electron microscopy

The total body weight of each mouse and tumor size were measured every week by a single observer. The tumor volume was calculated as follows: $V = 1/2 \text{ length}^2 \times \text{width}$ in units of mm^3. Animals were sacrificed after 7 days of treatment, and the tumors were removed; a portion of each tumor was placed in formalin, and the remainder was fresh-frozen in liquid nitrogen for further evaluation by transmission electron microscopy.

Statistical analysis

Data were processed with analysis of variance of repeated measurement, one-way analysis of variance, Dunnett's T3 and LSD test. *P* values were considered statistically significant when < 0.05. All statistical analyses were performed with SPSS software (version 19; SPSS, Chicago, IL, USA).

Results

Autophagy, apoptosis, and cell viability induced by NVP-BEZ235 in MM cell lines

The effects of NVP-BEZ235 on the viability of U266, KM3 and RPMI8226 MM cells are shown in **Figure 1A**, **1B**. Human myeloma cell lines U266, KM3 and RPMI8226 were treated with NVP-BEZ235 at different concentrations (0, 100 nM, 200 nM, 300 nM, 400 nM) for 0, 12, 24, 48 and 72 h. Cell viability was measured by MTT assay. NVP-BEZ235 induces ultrastructural features of autophagy. KM3 cells were treated with NVP-BEZ235 for 12 h and processed for electron microscopy. Acridine orange was used to stain AVOs in untreated or NVP-BEZ235 (50, 100 nM)-treated U266, KM3 and RPMI8226 cells for 12 h (**Figure 1C**). The cells were visualized under a red filter fluorescence microscope (**Figure 1D**). Autophagy bubble ratios were measur ed by flow cytometry. The effects of NVP-BEZ235 on the expression of LC3II and Atg5 in MM cells are shown in **Figure 1E**. Cells were treated with 50 nM and 100 nM NVP-BEZ235 for 12 h and LC3II, and Atg5 expression levels in U266, KM3 and RPMI8226 cells were evaluated using Western blot analysis. The results showed that the NVP-BEZ235 treatment of U266, KM3 and RPMI8226 cells reduced cell viability in a dose- and time-dependent manner. Autophagy bubbles with double membranes were observed in myeloma cells treated with NVP-BEZ235. Acridine orange staining and flow cytometry were used to measure the autophagy levels in untreated or BEZ235-treated myeloma cells. The results revealed that the autophagy cell ratio was higher in the NVP-BEZ235 group than in the control group. The treatment of myeloma cells with NVP-BEZ235 affected the expression of light chain 3 (LC3) and Atg5 proteins involved in the process of cellular autophagy. Hoeschst33258 staining (**Figure 2A**) and the flow cytometric analysis (**Figure 2B**) revealed that the NVP-BEZ235 treatment increased the rate of apoptosis of myeloma cells.

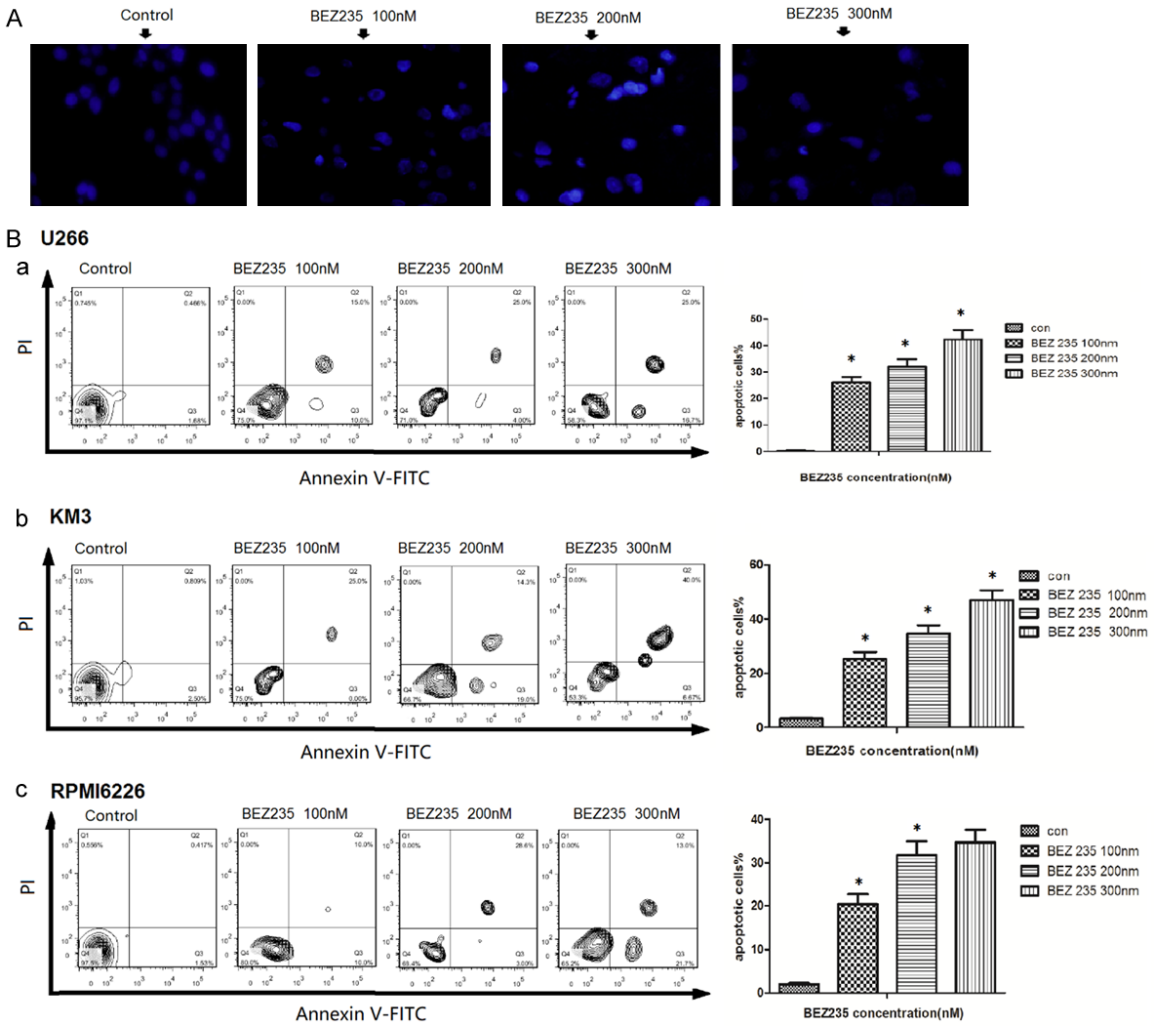

Figure 2. Autophagy induced by NVP-BEZ235 on MM cell lines. A. NPV-BEZ235 induced apoptosis in U266 cell lines. Apoptotic cell death was revealed by Hoechst 33258 staining with increasing NPV-BEZ235 (0, 100, 200 and 300 nmol/L) treatment for 48 h. Apoptotic cells exhibited highly condensed and fragmented nuclei morphology. B. NPV-BEZ235 induced apoptosis in U266, KM3 and RPMI8226 cell lines. Apoptotic cell death was revealed by Annexin V-FITC/PI staining with increasing NPV-BEZ235 (100, 200 and 300 nmol/L) treatment for 48 h. Early apoptotic cells are Annexin V-FITC+/PI- while late apoptotic cells are Annexin V-FITC+/PI+. The percentage of apoptotic cells is represented in the histogram.

The role of autophagy in multiple myeloma cell inhibition and apoptosis induced by NVP-BEZ235

NVP-BEZ235 in combination with CQ, 3-MA and BafA1 exerts enhanced effects in terms of inhibiting the viability of U266, KM3 and RPMI8226 MM cells. Human myeloma cell lines U266, KM3 and RPMI8226 were treated with NVP-BEZ235 in combination with CQ, 3-MA and BafA1. Cell viability was measured by MTT assay. The results of treatment for 48 hours with NVP-BEZ235 (12.5 nM, 25 nM, 50 nM, 100 nM) in combination with CQ at different concentrations (5 nM, 10 nM, 20 nM, 40 nM) are shown in **Figure 3A**. Morphological and numerical changes in MM U266, KM3 and RPMI8226 cell colony formation by CQ or NVP-BEZ235 alone for 21 days by methylcellulose clonogenic assay, as detected by microscopy, are shown in **Figure 3B**. NVP-BEZ235 alone or in combination with ATG5-siRNA exerted enhanced effects on inhibiting the viability of U266 MM cells. Cell viability was measured by MTT assay (**Figure 3C**). Morphological and numerical changes in U266 cells colony forma-

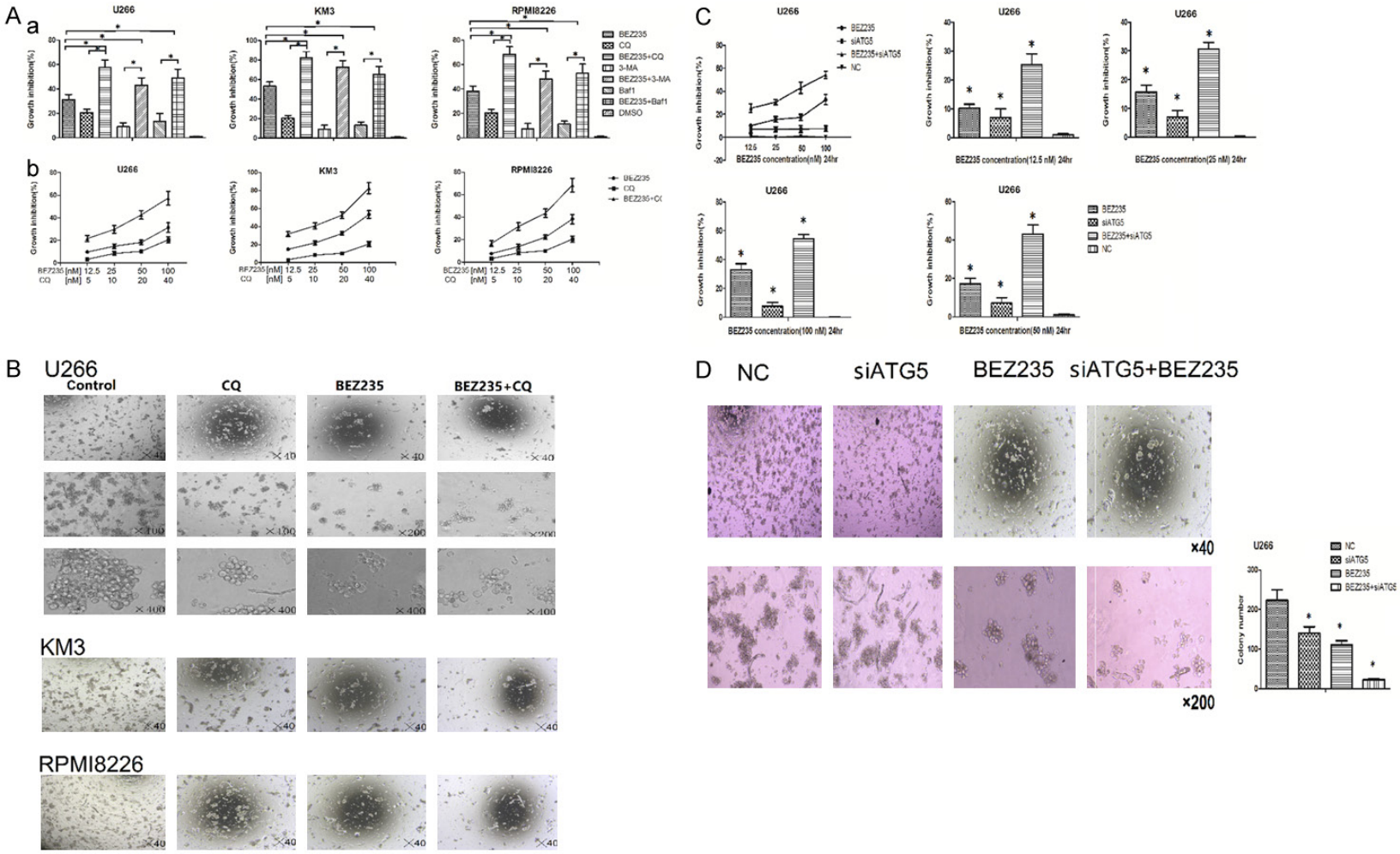

Figure 3. (A) NVP-BEZ235 in combination with CQ, 3-MA and BafA1 exerts enhanced effects on inhibiting the viability of U266, KM3 and RPMI8226 MM cells. (a) Human myeloma cell lines U266, KM3 and RPMI8226 were treated with NVP-BEZ235 (100 nM), CQ (40 nM), NVP-BEZ235+CQ, 3-MA (10 mM), NVP-BEZ235+3-MA, BafA1 (100 nM), NVP-BEZ235+BafA1 and DMSO for 48 h. Cell viability was detected by MTT assay. (b) NVP-BEZ235 (12.5 nM, 25 nM, 50 nM, 100 nM) in combination with CQ (5 nM, 10 nM, 20 nM, 40 nM) at different concentrations for 48 h. (B) Morphological and numerical changes of MM U266, KM3 and RPMI8226 cell colony formation by CQ (40 nM), NVP-BEZ235 (100 nM) and NVP-BEZ235+CQ for 21 days, detected by methylcellulose clonogenic assay under microscopy (C) NVP-BEZ235 alone (12.5 nM, 25 nM, 50 nM, 100 nM) or in combination with ATG5-siRNA exerts enhanced effects on inhibiting the viability of U266 MM cells for 24 h. Cell viability was detected by MTT assay. (D) Morphological and numerical changes of U266 cell colony formation by siAtg5, NVP-BEZ235 and NVP-BEZ235+ siAtg5 for 14 days, detected by methylcellulose clonogenic assay under microscopy. *Means significant difference was observed between the treated group and control group ($P < 0.05$).

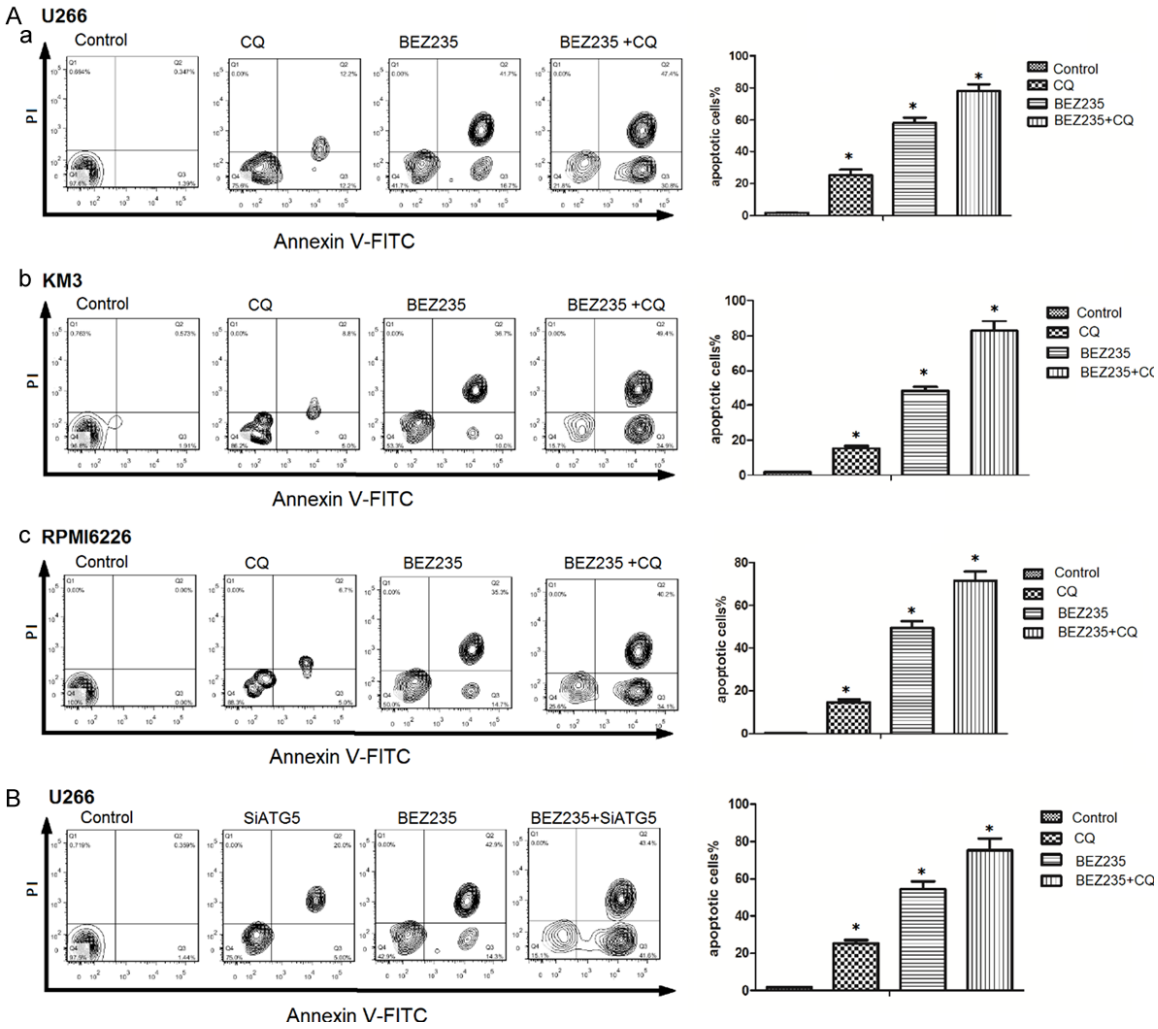

Figure 4. A. Chloroquine enhanced the apoptosis induced by NVP-BEZ235 in U266, KM3 and RPMI8226 cell lines. Apoptotic cell death was revealed by Annexin-V-FITC/PI staining with CQ (40 nM), NVP-BEZ235 (100 nM) and NVP-BEZ235+CQ treatment in U266, KM3 and RPMI8226 cell lines for 48 h. B. SiAtg5 enhanced the apoptosis induced by NVP-BEZ235 in U266 cell lines. Apoptotic cell death was revealed by Annexin-V-FITC/PI staining with siAtg5, NVP-BEZ235 (100 nM) and siAtg5+NVP-BEZ235 treatment for 48 h.

tion by SiAtg5 or NVP-BEZ235 alone for 14 days by methylcellulose clonogenic assay, as detected by microscopy, are shown in **Figure 3D**. Increased apoptotic cell death was revealed by Hoechst 33258 staining with an increasing concentration of NVP-BEZ235 (0, 100, 200 and 300 nmol/L) treatment for 48 h. Apoptotic cells exhibited highly condensed and fragmented nuclear morphology. Apoptotic cell death was revealed by Annexin-V-FITC/PI staining with increasing BEZ235 (100, 200 and 300 nmol/L) concentrations for 48 h. Apoptotic cells exhibited highly condensed and fragmented nuclear morphology. Chloroquine enhanced the apoptosis induced by NVP-BEZ235 in the U266, KM3, and RPMI8226 cell lines. Apoptotic cell death was revealed by Annexin-V-FITC/PI staining after chloroquine and NVP-BEZ235 treatment for 48 h (**Figure 4A**). SiAtg5 enhanced the apoptosis induced by NVP-BEZ235 in the U266 cell lines (**Figure 4B**). Apoptotic cell death was revealed by Annexin-V-FITC/PI staining after SiAtg5 and NVP-BEZ235 treatment for 48 h. The autophagy inhibitors 3-MA, CQ and BafA1 were used to examine the role of autophagy in NVP-BEZ235-induced cell damage in myeloma cells. The combination NVP-BEZ235+3-MA showed a higher growth inhibition of myeloma cells than NVP-BEZ235 alone. A similar result was observed in myeloma treated with the combinations NVP-BEZ235+CQ and NVP-BEZ235+BafA1. We also assessed the levels of

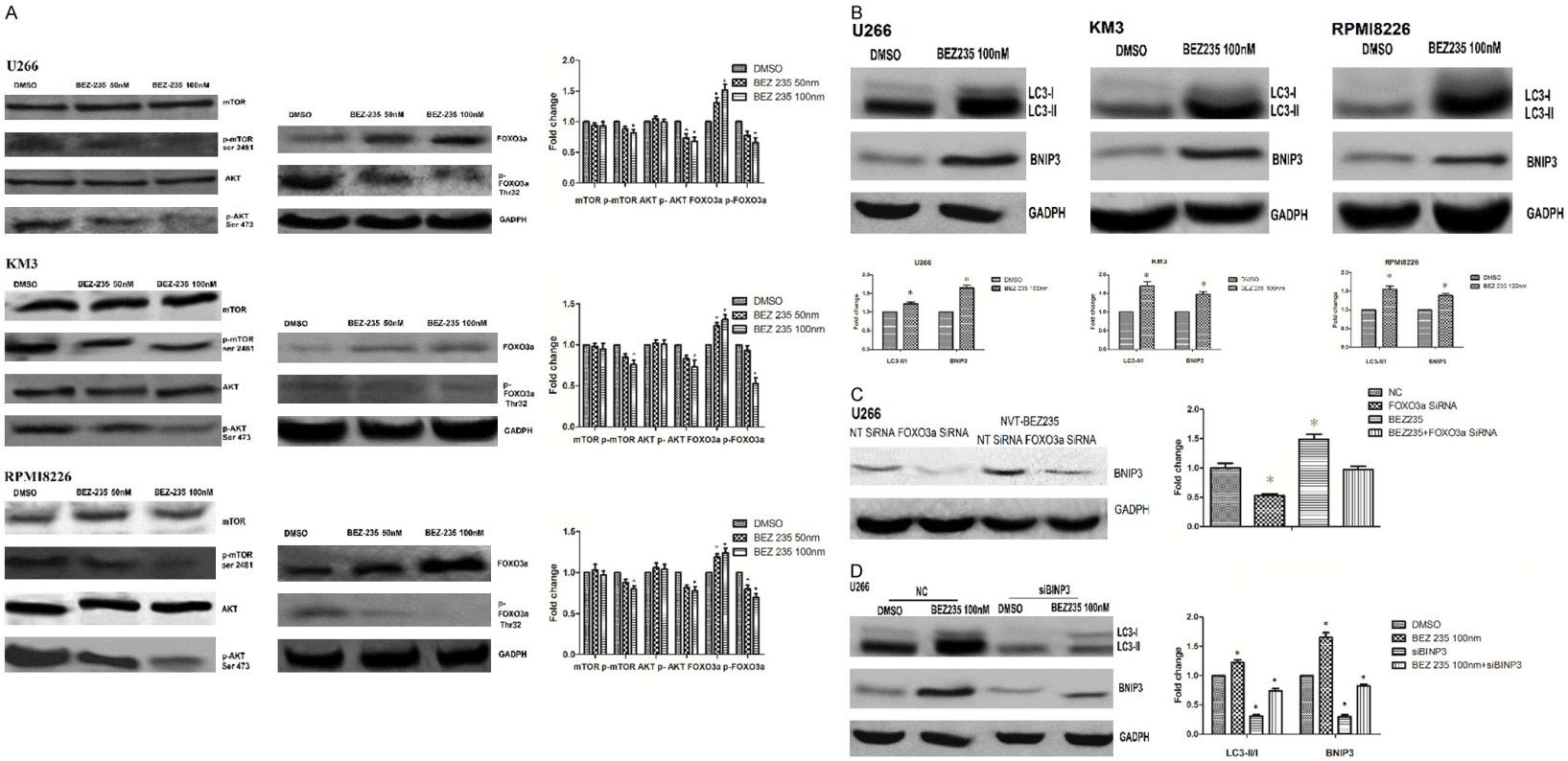

Figure 5. A. Effects of NVP-BEZ235 on the expression of mTOR2-Akt pathway proteins and FOXO3a in U266, KM3 and RPMI8226 cells. Cells were treated with 0 nM, 50 nM and 100 nM NVP-BEZ235 for 12 h and the mTOR, p-mTOR (ser 2481), AKT, p-AKT, FOXO3a and p-FOXO3a (Thr32) protein expression and the fold change in U266, KM3 and RPMI8226 cells was tested using Western blot analysis. B. Effects of NVP-BEZ235 (100 nM) on the expression of BNIP3 proteins and the fold change in U266, KM3 and RPMI8226 cells. Cells were treated with 100 nM NVP-BEZ235 for 12 h and BNIP3 and LCII protein expression was tested using Western blot analysis. C. Effects of NVP-BEZ235 (100 nM) and/or siFOXO3a on the expression of BNIP3 proteins and the fold change in U266 cells. D. Effects of NVP-BEZ235 (100 nM) and/or siBNIP3 on the expression of BNIP3 and LCII proteins. *Means significant difference was observed between the treated group and control ($P < 0.05$).

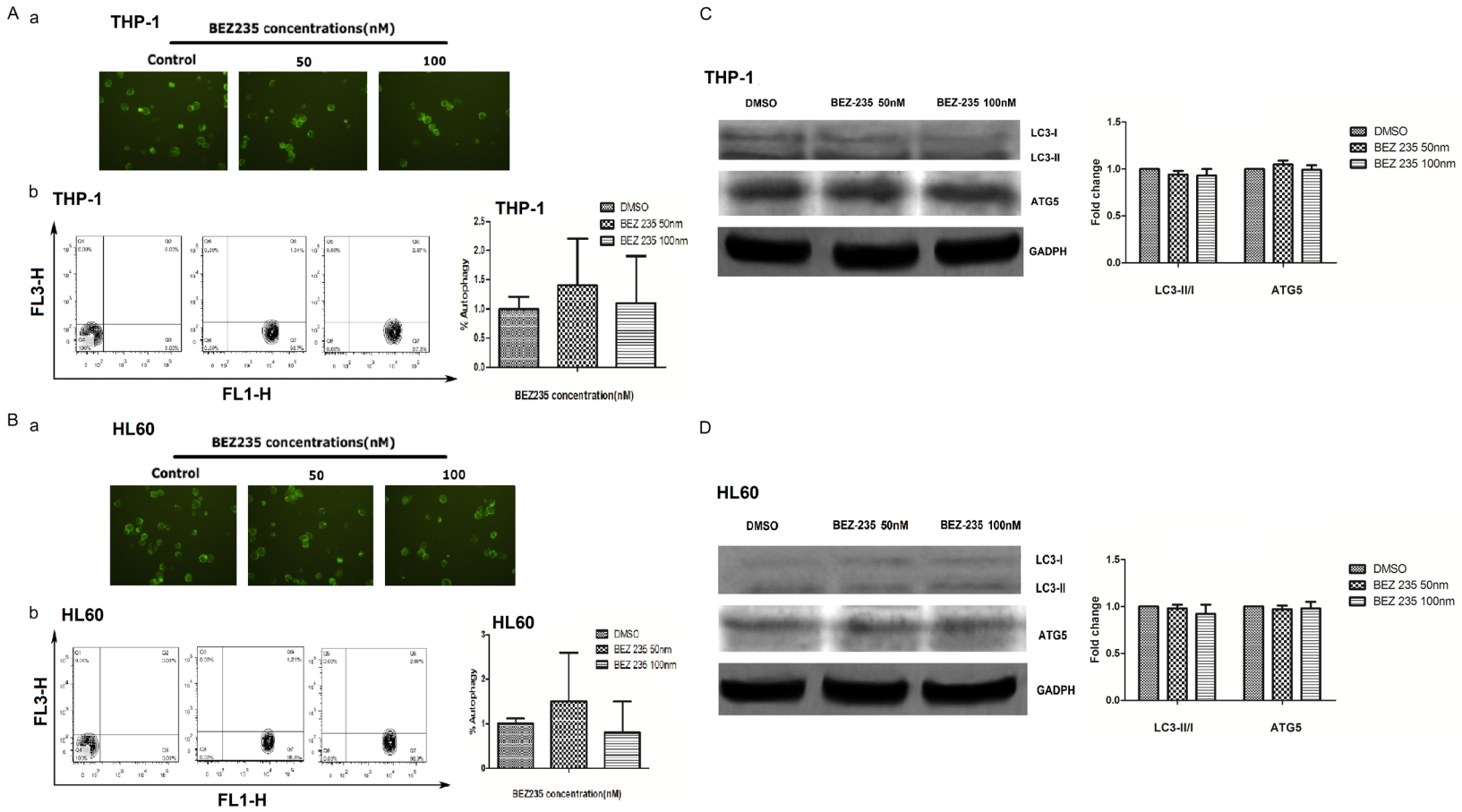

Figure 6. NVP-BEZ235 induced autophagy in MM cells selectively. (A) Acridine orange was used to stain AVOs in untreated or BEZ235 (50, 100 nM)-treated THP-1 cells for 12 h. (a) The cells were visualized under a red filter fluorescence microscope. (b) The cells were detected by flow cytometry. Autophagic ratio was calculated by measuring red/green fluorescence ratio. (B) Acridine orange was used to stain AVOs in untreated or BEZ235 (50, 100 nM)-treated HL60 cells for 12 h. The cells were visualized by (a) red filter fluorescence microscope (b) flow cytometry. Autophagic ratio was calculated by measuring red/green fluorescence ratio. (C) Effects of NVP-BEZ235 on the expression of LC3II and Atg5 in THP-1 cells. Cells were treated with 0 nM, 50 nM and 100 nM NVP-BEZ235 for 12 h and LC3II and Atg5 expression and the fold change in THP-1 cells was detected using Western blot analysis. (D) Effects of NVP-BEZ235 on the expression of LC3II and Atg5 in HL-60 cells. Cells were treated with 0 nM, 50 nM and 100 nM NVP-BEZ235 for 12 h and LC3II and Atg5 expression and the fold change in HL60 cells was measured by Western blot analysis. *Means significant difference was observed between the treated group and control ($P < 0.05$).

Table 1. Clinical features of the three multiple myeloma patients

Clinical features	Patient 1	Patient 2	Patient 3
Age/sex	61/F	70/F	62/F
M component	IgG κ	IgA λ	IgG κ
Durie-Salmon staging system	IIIB	IIIA	IIB
Hb (g/dL)	7.1	7.8	9.2
β2-microglobulin (mg/L)	4.6	5.1	2.4
plasma cells in BM%	30	31	18
calcium (mmol/L)	2.4	2.2	1.7
Serum M protein level	51	52	28

cell colony formation by myeloma cells treated with NVP-BEZ235 alone and NVP-BEZ235+CQ. The combination NVP-BEZ235+CQ showed lower cell colony formation of myeloma cells than NVP-BEZ235 alone. Similarly, the combination of NVP-BEZ235 and siAtg5 transfection showed a higher growth inhibition of myeloma cells and lower cell colony formation by myeloma cells than NVP-BEZ235 alone. The autophagy inhibitors 3-MA, CQ and BafA1 were used to examine the role of autophagy in NVP-BEZ235-induced apoptosis in myeloma cells. The combination of NVP-BEZ235+CQ showed higher growth inhibition of myeloma cells than NVP-BEZ235 alone. Similarly, the combination of NVP-BEZ235 and siAtg5 transfection showed higher growth inhibition of myeloma cells and lower cell colony formation of myeloma cells than NVP-BEZ235 alone.

The mechanism of the role of autophagy in multiple myeloma cells inhibition induced by NVP-BEZ235

The effects of NVP-BEZ235 on the expression of mTOR2-Akt pathway proteins and FOXO3a in myeloma cells were examined. Cells were treated with 50 nM and 100 nM NVP-BEZ235 for 12 h and mTOR, p-mTOR (ser2481), AKT, p-AKT, FOXO3a and p-FOXO3a (Thr32) protein expression in U266 cells was evaluated using Western blot analysis. Subsequently, the effects of NVP-BEZ235 and/or siFOXO3a on the expression of BNIP proteins in MM cells and the effects of NVP-BEZ235 on the expression of BNIP3 and LCII proteins in cells transfected with siBNIP3 were examined. Cells were treated with 100 nM NVP-BEZ235 for 12 h, and BNIP3 and LCII protein expressions in U266 cells was evaluated using Western blot analysis. The results showed that the NVP-BEZ235 group had significantly higher FOXO3a and BNIP protein levels and lower p-mTOR (ser2481), p-AKT, and p-FOXO3a (Thr32) protein levels than the control group. After treatment with NVP-BEZ235 and/or siFOXO3a, the BNIP3 protein level of the siFOXO3a cells decreased in the siFOXO3a group and increased in the NVP-BEZ235 group relative to the control group. After treatment with NVP-BEZ235 and/or siBNIP3, the BNIP3 and LCII protein levels were lower in the NVP-BEZ235 group than in the control group (**Figure 5**).

NVP-BEZ235 induced autophagy in MM cells selectively

Acridine orange was used to stain AVOs in untreated or BEZ235 (50, 100 nM)-treated THP-1 and HL60 cells for 12 h. The cells were visualized under a red filter fluorescence microscope. The autophagy bubble ratios were detected by flow cytometry. The effects of NVP-BEZ235 on the expression of LC3II and Atg5 in THP-1 cells were examined. Cells were treated with 50 nM and 100 nM NVP-BEZ235 for 12 h; LC3II and Atg5 expression in THP-1 and HL60 cells was evaluated using Western blot analysis. Acridine orange staining and flow cytometry were used to measure the autophagy levels of untreated or BEZ235 (50, 100 nM)-treated THP-1 and HL60 cells; LC3II and Atg5 expression levels were evaluated using Western blot analysis. There is no proof of autophagy occurrence in THP-1 and HL60 cells treated with NVP-BEZ235 (**Figure 6**).

The study of the autophagy and cell viability induced by NVP-BEZ235 on primary CD138+ myeloma cells

Primary CD138+ myeloma cells in bone marrow were analyzed by cell sorting. Clinical features of the three multiple myeloma patients are shown in **Table 1**. The effects of NVP-BEZ235 on the viability of primary myeloma cells were examined. Primary myeloma cells were treated with NVP-BEZ235 at different concentrations for different times. Cell viability was measured by MTT assay. Patients' MM cells were treated with NVP-BEZ235 for 12 h and processed for electron microscopy. The

Table 2. The relative expression levels of ATG5, FOXO3a and BNIP3 genes in CD138+ cells from no 1 patient before and after NVP-BEZ235 treatment

mRNA relative expression levels %	Control group	BEZ235 group	T value	*P* value
ATG5	0.901 ± 0.089	1.458 ± 0.046	-9.566	0.002
FOXO3a	0.921 ± 0.137	2.61 ± 0.111	-16.596	0.000
BNIP3	0.953 ± 0.047	2.012 ± 0.126	2.528	0.002

Table 3. The relative expression levels of ATG5, FOXO3a and BNIP3 genes in CD138+ cells from no 2 patient before and after NVP-BEZ235 treatment

mRNA relative expression levels %	Control group	BEZ235 group	T value	*P* value
ATG5	0.94 ± 0.087	1.684 ± 0.113	-9.037	0.001
FOXO3a	0.871 ± 0.206	1.78 ± 0.114	-6.681	0.003
BNIP3	0.864 ± 0.151	2.028 ± 0.061	-12.403	0.002

Table 4. The relative expression levels of ATG5, FOXO3a and BNIP3 genes in CD138+ cells from no 3 patient before and after NVP-BEZ235 treatment

mRNA relative expression levels %	Control group	BEZ235 group	T value	*P* value
ATG5	0.778 ± 0.207	1.723 ± 0.115	-6.925	0.005
FOXO3a	0.832 ± 0.229	1.639 ± 0.302	-3.682	0.021
BNIP3	0.843 ± 0.151	2.002 ± 0.265	-6.584	0.006

relative expression levels of ATG5, FOXO3a and BNIP3 genes in CD138+ cells before and after NVP-BEZ235 treatment, as measured by qRT-PCR, are shown in **Tables 2**-**4**. Bone marrow mononuclear cell separation in patients with multiple myeloma was performed. Western blot analysis of the effects of NVP-BEZ235 on the expression levels of the LC3-II/I, ATG5, FOXO3a, p-FOXO3a and BNIP3 proteins in patient MM cells indicated that the NVP-BEZ235 treatment of primary CD138+ myeloma cells reduced cell viability in a dose- and time-dependent manner. Autophagy bubbles with double membranes were observed under the electron microscope in primary myeloma cells treated with NVP-BEZ235. The relative expression levels (by qRT-PCR) of the ATG5, FOXO3a and BNIP3 genes in CD138+ cells from patients were significantly higher with NVP-BEZ235 treatment than with control treatment. The expression levels of the LC3-II/I, ATG5, FOXO3a, and BNIP3 proteins in the patients' MM cells were significantly higher with NVP-BEZ235 treatment than in the control group. The expression of p-FOXO3a proteins in the patients' MM cells was significantly lower with NVP-BEZ235 treatment than with control treatment (**Figure 7**).

The study of the autophagy and tumor proliferation inhibition induced by NVP-BEZ235 on u266 myeloma tumor-burdened nude mice

We established an animal model of u266 myeloma tumor-burdened nude mice. We compared the general conditions, animal body weights and sizes of the tumors and calculated the tumor volume inhibition rates, to verify whether NVP-BEZ235 myeloma cells induced autophagy in tumor-burdened nude mice, as visualized by transmission electron microscopy. There was no significant difference between the animal body weights of the NVP-BEZ235 group and control group. The sizes of the tumors decreased in the NVP-BEZ235 group compared to the control group; the tumor growth inhibition rate was 83.33% (± 6.50%). Autophagy bubbles with double membranes were observed in primary myeloma cells in vivo in myeloma mice treated with NVP-BEZ235 (**Figure 8**).

Discussion

NVP-BEZ235, a novel, dual class I PI3K/mTOR inhibitor, is an imidazoquinoline derivative [21]. NVP-BEZ235 binds to the ATP-binding clefts of PI3K and mTOR kinase, thereby inhibiting their

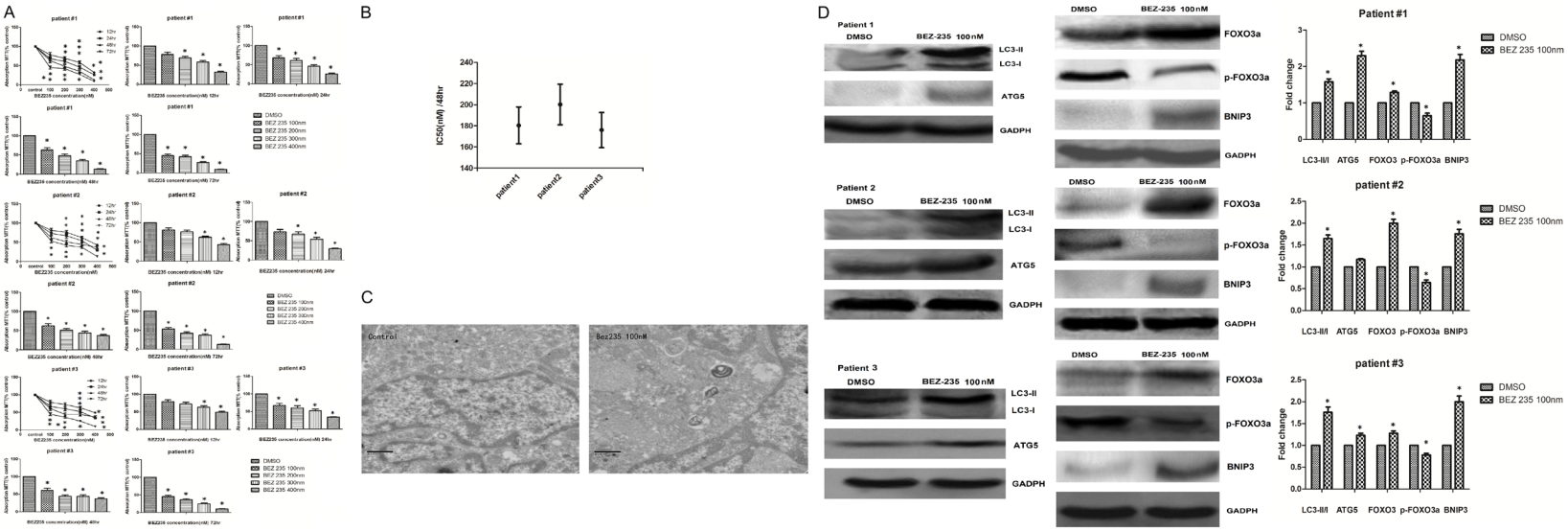

Figure 7. A. Effects of NVP-BEZ235 on viability of Human myeloma cells derived from three patients. Human myeloma cells derived from three patients were treated with NVP-BEZ235 at different concentrations (0, 100 nM, 200 nM, 300 nM, 400 nM) for 0, 12, 24, 48 and 72 h. Cell viability was detected by MTT assay. *Means significant difference was observed between the treated group and control ($P < 0.05$). B. IC50 of NVP-BEZ235 in 3 patients' primary MM cells at 48 hr. C. BEZ235 (100 nM) induces ultrastructural features of autophagy. Patients' primary MM cells were treated with NVP-BEZ235 for 12 h and observed under electron microscopy. D. Effects of NVP-BEZ235 (100 nM) on the expression and the fold change of LC3-II/I, ATG5, FOXO3a, p-FOXO3a and BNIP3 proteins in patients' MM cells. *Means significant difference was observed between the treated group and control ($P < 0.05$).

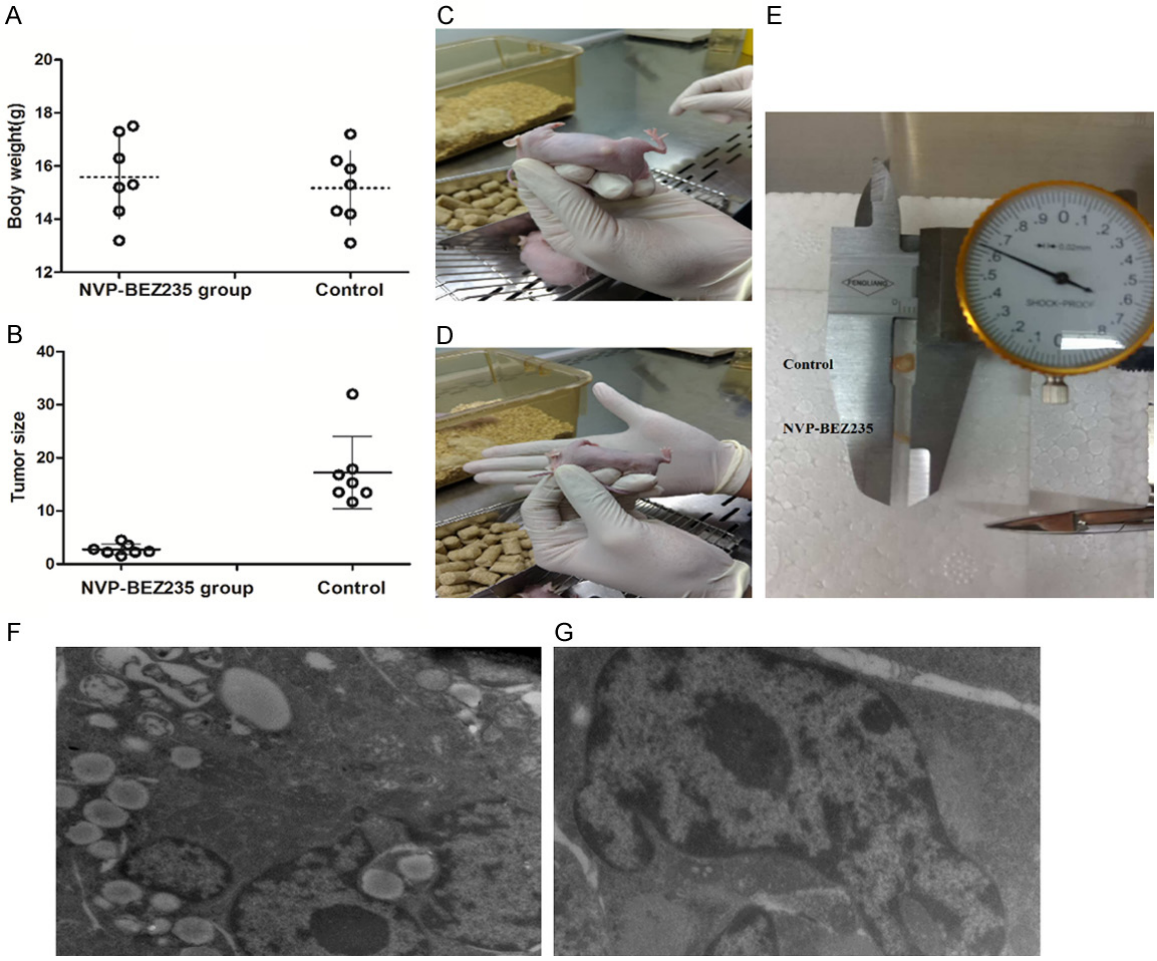

Figure 8. Tumor suppression of NVP-BEZ235 in tumor-burdened nude mice. The animal model of u266 myeloma cell tumor-burdened nude mice was established. Nude mice of the control group were given an oral administration of solvent while the NVP-BEZ235 group was given an oral administration NVP-BEZ235 (30 mg/mL (NMP+PEG 300 (10+90, v+v) (45 mg/kg p.o. q.d.)) for 7 consecutive 7 days. At day 8 (A) Animal body weight of the NVP-BEZ235 group and control group were measured. (B) Volume of the tumors was calculated: V = 1/2 length^2 × width in units of mm3. The tumor growth inhibition rate (IR) was calculated using the formula IR (%) = (1-TWt/TWc) × 100, where TWt and TWc are the mean tumor weight of treated and control groups, respectively. (C) Mice in the control group on day 7 (D) Mice in NPV-BEZ235 group on day 7. (E) Tumor from NVP-BEZ235 group and the control group on day 8. (F) The tumors in NVP-BEZ235 group were processed for electron microscopy and the characteristic double-membrane structure of autophagosomes were observed. (G) The tumors in the control group were processed for electron microscopy.

activities. Increasing evidence shows that NVP-BEZ235 is able to effectively and specifically reverse the hyperactivation of the PI3K/mTOR pathway, resulting in potent antiproliferative and antitumor activities in a broad range of cancer cell lines and experimental tumors. The mTOR kinase pathway plays an important role in autophagy and antiproliferation [19, 20]. mTOR kinase simultaneously senses signals from energy, cell growth and division, oxygen levels, stress and nutrients and then regulates cell growth during early development and cell aging. Attenuated insulin-IGF1 signaling, nutrient or energy limitation and stress all repress mTORC1 activity. Inhibition of PI3K/AKT/mTOR signaling can not only decrease the proliferation of tumor cells but also induce autophagy. Autophagy is an essential catabolic process that maintains cellular homeostasis by regulation of cell survival and death and reduces diverse stresses through lysosomal recycling of the unnecessary and damaged cell components. The PI3K/AKT/mTOR pathway, one of the important regulators of autophagy, is the major inhibitory signal that shuts off autophagy in the presence of growth factors and abundant

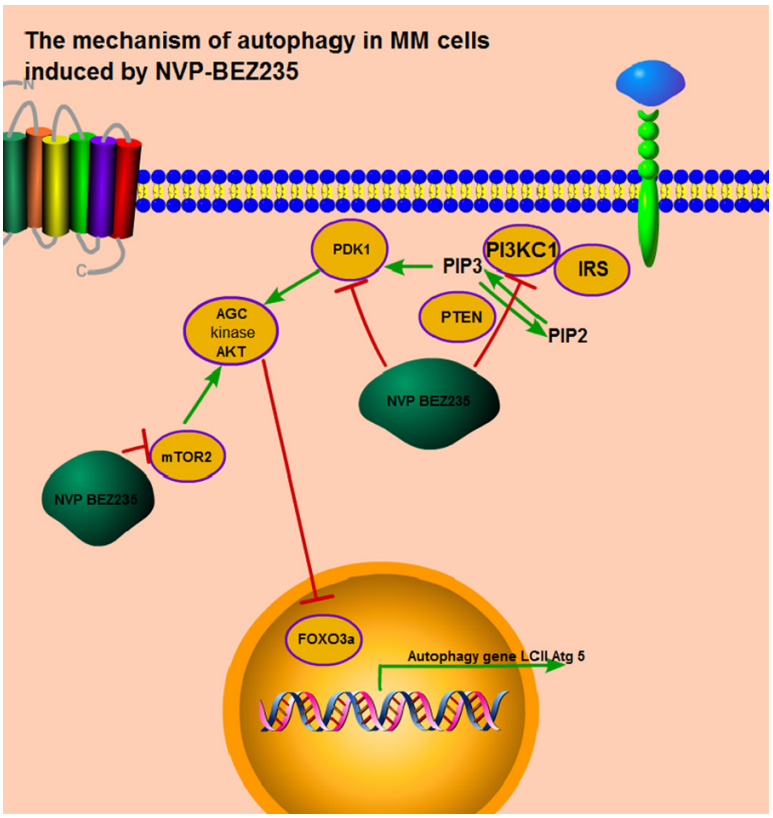

Figure 9. The mechanisms of autophagy in MM cells induced by NVP-BEZ235. The FoxO3a is regulated by the PI3K/Akt signaling pathway and directs an autophagy program in MM cells after the treatment of NVP-BEZ235. NVP-BEZ235 induced autophagy through the mTOR2-Akt-FOXO3a-BNIP3 pathway in MM cells.

nutrients. Accordingly, inhibition of dual class I PI3K/mTOR signaling by the inhibitor NVP-BEZ235 induces autophagy in a panel of cancer cells, including human lung cancer, as well as prostate cancer and colorectal cancer cells [4, 22-25]. In the present study, we also found that NVP-BEZ235 causes significant autophagy in U266, KM3 and RPMI8226 cells, human myeloma cells derived from three patients and MM tumor-burdened nude mice, evidenced by detection of cells stained with AO under a red filter fluorescence microscope or by flow cytometry, double membrane structure of the autophagic vacuoles by transmission electron microscope, and increased levels of the LC3B-II/I ratio. Not surprisingly, autophagy was induced by NVP-BEZ235, a dual PI3K/mTOR inhibitor because mTOR acts as a negative regulator of autophagy.

The role of autophagy in cell death or apoptosis is controversial. Generally, it appears that apoptosis and autophagy exhibit some degree of mutual inhibition [26, 27]. On most occasions, autophagy raises the threshold of stress required to induce apoptosis or suppresses apoptosis directly, which means that autophagy tends to be anti-apoptotic instead of pro-apoptotic. Amaravadi et al. indicated that autophagy and apoptosis play opposing roles in cancer cells in chronic myelogenous leukemia (CML) cell lines and have reported findings that inhibition of autophagy with 3MA and/or chloroquine sensitizes apoptosis-resistant CML tumor cells to cancer treatment [28]. Han et al. showed that TRAIL treatment resistance in Hct116 colon carcinoma cells may be partly attributed to the cytoprotective effects of autophagy. These cancer cells, which overexpress c-FLIP and are resistant to TRAIL-mediated apoptosis, show enhanced Beclin-1 expression and raised autophagosome formation under TRAILRs or Fas stimulation [29]. Huang and Sinicrope observed that COX-2 inhibitor celecoxib-induced apoptosis was enhanced by ABT-737 and by inhibition of autophagy in human colorectal cancer cells [30]. Han et al. showed that EGFR tyrosine kinase inhibitors gefitinib and erlotinib activated autophagy as a cytoprotective response in human lung cancer cells [31]. Wang et al. demonstrated quercetin-induced protective autophagy in gastric cancer cells and the involvement of Akt-mTOR- and hypoxia-induced factor 1α-mediated signaling. In most cases, autophagy shuts off the induction of apoptosis, and apoptosis-associated caspase blocks activation the autophagic process [32]. It is only in rare cases that autophagy or autophagy-relevant proteins induce apoptosis or necrosis, degrading the cytoplasm excessively and resulting in 'autophagic cell death' (ACD). In our current study, NVP-BEZ235 induced apoptosis and autophagy at the same time in MM cells.

The dual class I PI3K/mTOR inhibitor-induced apoptosis was enhanced by autophagy inhibitors CQ, 3-MA and BafA1 by MTT assay and methylcellulose clonogenic assay in human multiple myeloma cells. Similar effects were observed in MM cells with the inhibition of small interfering RNA targeting Atg5 (siAtg5) by MTT assay and methylcellulose clonogenic assay. The anti-apoptotic effects of autophagy induced by NVP-BEZ235 on human MM cells are similar to those reported in the previous literature.

However, what remained unanswered is the mechanism of autophagy in MM cells induced by NVP-BEZ235. We, therefore, explored the downstream pathways. FoxO3a belongs to the mammalian Forkhead box O (FoxO) subfamily, which includes the human homologs of the *C. elegans* transcription factor DAF-16 and has two domains: one winged-helix domain and one highly conserved 110-amino acid DNA binding [33, 34]. As a major member of FoxO, FoxO3a is regulated by the PI3K/Akt signaling pathway. Recent studies have demonstrated that FoxO3a regulates a wide variety of cell functions including proliferation, apoptosis, aging, stress-resistance, cell cycle arrest, tumor suppression and autophagy by regulating gene expression [35-38]. By and large, FoxO3a helps to suppress cell cycle progression and accelerate cell death. Thus, FoxO3a has been thought to be a critical protein to restrain cancer cell progression. Recent research has also shown that FoxO3a has some additional functions, such as stress response, longevity and autophagy induction, to protect cells from environmental stresses [36, 39-42]. Warr MR et al. discovered that FoxO3a directs a protective autophagy program in hematopoietic stem cells. In their study, they demonstrated that, in contrast to the short-lived myeloid progeny, HSCs induce autophagy intensely after cytokine withdrawal ex vivo and energy restriction in vivo. They also showed that FoxO3a is an important factor to maintain a gene expression program that rapidly induce autophagy in HSCs under the environment of starvation [43]. In our present study, we detected the expression of mTOR2-Akt pathway proteins and FOXO3a proteins following NVP-BEZ235 treatment in myeloma cells as well as the mTOR2-Akt pathway genes and FOXO3a genes in primary myeloma cells from patients. The results showed that the NVP-BEZ235 group had significantly higher FOXO3a protein levels and lower p-mTOR (ser2481), p-AKT, p-FOXO3a (Thr32) protein levels than the control group. Similarly, the relative expression of the FOXO3a gene in CD138+ cells from patients was significantly higher with NVP-BEZ235 than with the control treatment by qRT-PCR. The NVP-BEZ235 group had significantly higher FOXO3a protein levels and lower p-FOXO3a protein levels than the control group. Furthermore, we explored the role of FOXO3a in the autophagy induced by NVP-BEZ235 in MM cells. We transfected small interfering RNA targeting FOXO3a (siFOXO3a) and measured the expression levels of the autophagy-associated proteins BNIP3 in MM cells and found that the NVP-BEZ235 group had a significantly higher BNIP3 protein level than the control group. Additionally, we observed higher relative expression levels of BNIP3 genes in CD138+ cells from patients in the NVP-BEZ235 group than from those in the control group. We also analyzed the role of BNIP3 in the autophagy induced by NVP-BEZ235 in MM cells. We transfected small interfering RNA targeting BNIP3 (siBNIP3). The results showed that after the transfection of siBNIP3, the BNIP3 and LCII protein levels were lower in the NVP-BEZ235 group than in the control group (**Figure 9**). All of these findings highlight that FoxO3a is regulated by the PI3K/Akt signaling pathway and directs the autophagy program in MM cells after the treatment of NVP-BEZ235. NVP-BEZ235 induces autophagy through the mTOR2-Akt-FOXO3a-BNIP3 pathway in MM cells.

Acknowledgements

This study was supported by grants from the Natural Science Foundation of Zhejiang province (No. LQ16H080002) and the National Natural Science Foundation (No. 81600167).

Disclosure of conflict of interest

None.

Abbreviations

PI3K, Phosphatidylinositol 3-kinase; Akt, Serine/threonine Kinase; mTOR, Mammalian Target Of Rapamycin; S6K, ribosomal S6 kinase; 4E-BP1, eIF4E binding protein 1; MTT, methyl thiazolyl tetrazolium; Atg5, Autophagy protein

5; FOXO3, Forkhead box O3; BNIP3, BCL2-adenovirusE1B 19kD-interactingprotein 3; JAK, Janus Kinase; STAT, Signal transducers and activators of transcription.

Address correspondence to: Qifa Liu, Department of Hematology, Nanfang Hospital, Southern Medical University, Guangzhou, 510010, China. Tel: +862061641888; E-mail: liuqifa6281@163.com; Kang Yu, Department of Hematology, The First Affiliated Hospital of Wenzhou Medical University, 2 Nanbai Xiang, Wenzhou 325000, China. Tel: +86-577-55579489; Fax: +86577-55579489; E-mail: yukang1_2@126.com

References

[1] Shi Y, Daniels-Wells TR, Frost P, Lee J, Finn RS, Bardeleben C, Penichet ML, Jung ME, Gera J and Lichtenstein A. Cytotoxic properties of a DEPTOR-mTOR inhibitor in multiple myeloma cells. Cancer Res 2016; 76: 5822-5831.

[2] Gu Y, Kaufman JL, Bernal L, Torre C, Matulis SM, Harvey RD, Chen J, Sun SY, Boise LH and Lonial S. MLN4924, an NAE inhibitor, suppresses AKT and mTOR signaling via upregulation of REDD1 in human myeloma cells. Blood 2014; 123: 3269-3276.

[3] Xiang RF, Wang Y, Zhang N, Xu WB, Cao Y, Tong J, Li JM, Wu YL and Yan H. MK2206 enhances the cytocidal effects of bufalin in multiple myeloma by inhibiting the AKT/mTOR pathway. Cell Death Dis 2017; 8: e2776.

[4] Gan ZY, Fitter S, Vandyke K, To LB, Zannettino AC and Martin SK. The effect of the dual PI3K and mTOR inhibitor BEZ235 on tumour growth and osteolytic bone disease in multiple myeloma. Eur J Haematol 2015; 94: 343-354.

[5] Aronson LI, Davenport EL, Mirabella F, Morgan GJ and Davies FE. Understanding the interplay between the proteasome pathway and autophagy in response to dual PI3K/mTOR inhibition in myeloma cells is essential for their effective clinical application. Leukemia 2013; 27: 2397-2403.

[6] Stengel C, Cheung CW, Quinn J, Yong K and Khwaja A. Optimal induction of myeloma cell death requires dual blockade of phosphoinositide 3-kinase and mTOR signalling and is determined by translocation subtype. Leukemia 2012; 26: 1761-1770.

[7] Hoang B, Frost P, Shi Y, Belanger E, Benavides A, Pezeshkpour G, Cappia S, Guglielmelli T, Gera J and Lichtenstein A. Targeting TORC2 in multiple myeloma with a new mTOR kinase inhibitor. Blood 2010; 116: 4560-4568.

[8] Peterson TR, Laplante M, Thoreen CC, Sancak Y, Kang SA, Kuehl WM, Gray NS and Sabatini DM. DEPTOR is an mTOR inhibitor frequently overexpressed in multiple myeloma cells and required for their survival. Cell 2009; 137: 873-886.

[9] Frost P, Shi Y, Hoang B and Lichtenstein A. AKT activity regulates the ability of mTOR inhibitors to prevent angiogenesis and VEGF expression in multiple myeloma cells. Oncogene 2007; 26: 2255-2262.

[10] Shi Y, Frost P, Hoang B, Yang Y, Fukunaga R, Gera J and Lichtenstein A. MNK kinases facilitate c-myc IRES activity in rapamycin-treated multiple myeloma cells. Oncogene 2013; 32: 190-197.

[11] Hoang B, Benavides A, Shi Y, Yang Y, Frost P, Gera J and Lichtenstein A. The PP242 mammalian target of rapamycin mTOR inhibitor activates extracellular signal-regulated kinase ERK in multiple myeloma cells via a target of rapamycin complex 1 TORC1/eukaryotic translation initiation factor 4E eIF-4E/RAF pathway and activation is a mechanism of resistance. J Biol Chem 2012; 287: 21796-21805.

[12] Ghobrial IM, Weller E, Vij R, Munshi NC, Banwait R, Bagshaw M, Schlossman R, Leduc R, Chuma S, Kunsman J, Laubach J, Jakubowiak AJ, Maiso P, Roccaro A, Armand P, Dollard A, Warren D, Harris B, Poon T, Sam A, Rodig S, Anderson KC and Richardson PG. Weekly bortezomib in combination with temsirolimus in relapsed or relapsed and refractory multiple myeloma: a multicentre, phase 1/2, open-label, dose-escalation study. Lancet Oncol 2011; 12: 263-272.

[13] Farag SS, Zhang S, Jansak BS, Wang X, Kraut E, Chan K, Dancey JE and Grever MR. Phase II trial of temsirolimus in patients with relapsed or refractory multiple myeloma. Leuk Res 2009; 33: 1475-1480.

[14] Gunther A, Baumann P, Burger R, Kellner C, Klapper W, Schmidmaier R and Gramatzki M. Activity of everolimus RAD001 in relapsed and/or refractory multiple myeloma: a phase I study. Haematologica 2015; 100: 541-547.

[15] Yee AJ, Hari P, Marcheselli R, Mahindra AK, Cirstea DD, Scullen TA, Burke JN, Rodig SJ, Hideshima T, Laubach JP, Ghobrial IM, Schlossman RL, Munshi NC, Anderson KC, Weller EA, Richardson PG and Raje NS. Outcomes in patients with relapsed or refractory multiple myeloma in a phase I study of everolimus in combination with lenalidomide. Br J Haematol 2014; 166: 401-409.

[16] Koldehoff M, Beelen DW and Elmaagacli AH. Inhibition of mTOR with everolimus and silencing by vascular endothelial cell growth factor-specific siRNA induces synergistic antitumor activity in multiple myeloma cells. Cancer Gene Ther 2014; 21: 275-282.

[17] Massard C, Chi KN, Castellano D, de Bono J, Gravis G, Dirix L, Machiels JP, Mita A, Gonzalez BM, Turri S, Maier J, Csonka D, Chakravartty A and Fizazi K. Phase Ib dose-finding study of abiraterone acetate plus buparlisib BKM120 or dactolisib BEZ235 in patients with castration-resistant prostate cancer. Eur J Cancer 2017; 76: 36-44.

[18] Zhu Y, Tian T, Zou J, Wang Q, Li Z, Li Y, Liu X, Dong B, Li N, Gao J and Shen L. Dual PI3K/mTOR inhibitor BEZ235 exerts extensive antitumor activity in HER2-positive gastric cancer. BMC Cancer 2015; 15: 894.

[19] Cebulla J, Huuse EM, Pettersen K, van der Veen A, Kim E, Andersen S, Prestvik WS, Bofin AM, Pathak AP, Bjorkoy G, Bathen TF and Moestue SA. MRI reveals the in vivo cellular and vascular response to BEZ235 in ovarian cancer xenografts with different PI3-kinase pathway activity. Br J Cancer 2015; 112: 504-513.

[20] Yasumizu Y, Miyajima A, Kosaka T, Miyazaki Y, Kikuchi E and Oya M. Dual PI3K/mTOR inhibitor NVP-BEZ235 sensitizes docetaxel in castration resistant prostate cancer. J Urol 2014; 191: 227-234.

[21] Ma BB, Lui VW, Hui CW, Lau CP, Wong CH, Hui EP, Ng MH, Cheng SH, Tsao SW, Tsang CM, Cheung CS, Ho K and Chan AT. Preclinical evaluation of the mTOR-PI3K inhibitor BEZ235 in nasopharyngeal cancer models. Cancer Lett 2014; 343: 24-32.

[22] Scott EC, Maziarz RT, Spurgeon SE, Medvedova E, Gajewski J, Reasor-Heard S, Park B, Kratz A, Thomas GV, Loriaux M, Cascio M, Podolak J, Gordon M, Botelho J, Stadtmauer E, Amaravadi R and Vogl DT. Double autophagy stimulation using chemotherapy and mTOR inhibition combined with hydroxychloroquine for autophagy modulation in patients with relapsed or refractory multiple myeloma. Haematologica 2017; 102: e261-e265.

[23] Zhang LD, Liu Z, Liu H, Ran DM, Guo JH, Jiang B, Wu YL and Gao FH. Oridonin enhances the anticancer activity of NVP-BEZ235 against neuroblastoma cells in vitro and in vivo through autophagy. Int J Oncol 2016; 49: 657-665.

[24] Yu Y, Yu X, Ma J, Tong Y and Yao J. Effects of NVP-BEZ235 on the proliferation, migration, apoptosis and autophagy in HT-29 human colorectal adenocarcinoma cells. Int J Oncol 2016; 49: 285-293.

[25] Yang X, Niu B, Wang L, Chen M, Kang X, Wang L, Ji Y and Zhong J. Autophagy inhibition enhances colorectal cancer apoptosis induced by dual phosphatidylinositol 3-kinase/mammalian target of rapamycin inhibitor NVP-BEZ235. Oncol Lett 2016; 12: 102-106.

[26] Moscat J and Diaz-Meco MT. p62 at the crossroads of autophagy, apoptosis, and cancer. Cell 2009; 137: 1001-1004.

[27] Crighton D, Wilkinson S, O'Prey J, Syed N, Smith P, Harrison PR, Gasco M, Garrone O, Crook T and Ryan KM. DRAM, a p53-induced modulator of autophagy, is critical for apoptosis. Cell 2006; 126: 121-134.

[28] Amaravadi RK, Yu D, Lum JJ, Bui T, Christophorou MA, Evan GI, Thomas-Tikhonenko A and Thompson CB. Autophagy inhibition enhances therapy-induced apoptosis in a Myc-induced model of lymphoma. J Clin Invest 2007; 117: 326-336.

[29] Han J, Hou W, Goldstein LA, Lu C, Stolz DB, Yin XM and Rabinowich H. Involvement of protective autophagy in TRAIL resistance of apoptosis-defective tumor cells. J Biol Chem 2008; 283: 19665-19677.

[30] Huang S and Sinicrope FA. Celecoxib-induced apoptosis is enhanced by ABT-737 and by inhibition of autophagy in human colorectal cancer cells. Autophagy 2010; 6: 256-269.

[31] Han W, Pan H, Chen Y, Sun J, Wang Y, Li J, Ge W, Feng L, Lin X, Wang X, Wang X and Jin H. EGFR tyrosine kinase inhibitors activate autophagy as a cytoprotective response in human lung cancer cells. PLoS One 2011; 6: e18691.

[32] Wang K, Liu R, Li J, Mao J, Lei Y, Wu J, Zeng J, Zhang T, Wu H, Chen L, Huang C and Wei Y. Quercetin induces protective autophagy in gastric cancer cells: involvement of Akt-mTOR- and hypoxia-induced factor 1alpha-mediated signaling. Autophagy 2011; 7: 966-978.

[33] Wang Y, Mu Y, Zhou X, Ji H, Gao X, Cai WW, Guan Q and Xu T. SIRT2-mediated FOXO3a deacetylation drives its nuclear translocation triggering FasL-induced cell apoptosis during renal ischemia reperfusion. Apoptosis 2017; 22: 519-530.

[34] Zhang H, Zhao Z, Pang X, Yang J, Yu H, Zhang Y, Zhou H and Zhao J. MiR-34a/sirtuin-1/foxo3a is involved in genistein protecting against ox-LDL-induced oxidative damage in HUVECs. Toxicol Lett 2017; 277: 115-122.

[35] Choi S, Chung H, Hong H, Kim SY, Kim SE, Seoh JY, Moon CM, Yang EG and Oh ES. Inflammatory hypoxia induces syndecan-2 expression through IL-1beta-mediated FOXO3a activation in colonic epithelia. FASEB J 2017; 31: 1516-1530.

[36] Liu W, Wang X, Liu Z, Wang Y, Yin B, Yu P, Duan X, Liao Z, Chen Y, Liu C, Li X, Dai Y and Tao Z. SGK1 inhibition induces autophagy-dependent apoptosis via the mTOR-Foxo3a pathway. Br J Cancer 2017; 117: 1139-1153.

[37] Spinelli M, Fusco S, Mainardi M, Scala F, Natale F, Lapenta R, Mattera A, Rinaudo M, Li Puma DD, Ripoli C, Grassi A, D'Ascenzo M and Grassi C. Brain insulin resistance impairs hippocampal synaptic plasticity and memory by increasing GluA1 palmitoylation through Fox03a. Nat Commun 2017; 8: 2009.

[38] Stawski L, Marden G and Trojanowska M. The activation of human dermal microvascular cells by Poly I:C, lipopolysaccharide, imiquimod, and ODN2395 is mediated by the Fli1/FOXO3A pathway. J Immunol 2018; 1: 248-259.
[39] Chiacchiera F and Simone C. Inhibition of p38alpha unveils an AMPK-FoxO3A axis linking autophagy to cancer-specific metabolism. Autophagy 2009; 5: 1030-1033.
[40] Dai B, Zhu F, Chen Y, Zhou R, Wang Z, Xie Y, Wu X, Zu S, Li G, Ge J and Chen F. ASIC1a promotes acid-induced autophagy in rat articular chondrocytes through the AMPK/FoxO3a pathway. Int J Mol Sci 2017; 18: 2125.
[41] Liu Z, Wang Y, Zhao S, Zhang J, Wu Y and Zeng S. Imidazole inhibits autophagy flux by blocking autophagic degradation and triggers apoptosis via increasing FoxO3a-Bim expression. Int J Oncol 2015; 46: 721-731.
[42] Sanchez AM, Csibi A, Raibon A, Cornille K, Gay S, Bernardi H and Candau R. AMPK promotes skeletal muscle autophagy through activation of forkhead FoxO3a and interaction with Ulk1. J Cell Biochem 2012; 113: 695-710.
[43] Warr MR, Binnewies M, Flach J, Reynaud D, Garg T, Malhotra R, Debnath J and Passegue E. FOXO3A directs a protective autophagy program in haematopoietic stem cells. Nature 2013; 494: 323-327.